Available online at www.sciencedirect.com

ScienceDirect

Energy Procedia 6 (2011) 65–74

Energy Procedia

MEDGREEN 2011-LB

Computational modeling of the transport and electrochemical phenomena in solid oxide fuel cells

Hocine. Mahcene[a], Hocine Ben Moussa[b], Hamza. Bouguettaia[a], Djamel. Bechki[a], Mostefa Zeroual[c]. *a*

[a] *Laboratory of New and Renewable Energy (LENREZA), P.O.Box 511, Ouargla University 30000 Algeria*
[b] *Département de mécanique, Université de Batna, Algeria*
[c] *Département de physique, Université de Batna, Algeria*

Abstract

A mathematical model for a planar solid oxide fuel cell (SOFC) was constructed. The chemical species, the temperature distribution and the cell performance were calculated using unit model with double channels of co-flow pattern. The governing equations for mass continuity, momentum conservation, energy conservation and species conservation were discretized with the finite volume method. The equations are implemented in FORTRAN language. The water production and the hydrogen in the anode were taken into consideration in the model. The effects of the anode thickness, the operating conditions and various losses on the calculated results were investigated. Parametric analyses showed that all temperatures decreased with increasing losses. Another important finding is that the anode thickness has significant effect on gases distribution, along the main flow channel. For gas flow rate of $80.10^{-8}\ m^3\ s^{-1}$, *the peak power density was* $37508 Wm^{-2}$, *which was about 7.5% higher than that of* $80.10^{-9}\ m^3\ s^{-1}$ *gas flow rate. The results of this paper provide better understanding on the coupled heat/mass transfer and electrochemical reaction phenomena in an SOFC. The model developed can serve as a useful tool for SOFC design optimization*

© 2010 Published by Elsevier Ltd. Open access under CC BY-NC-ND license.
Selection and/or peer-review under responsibility of [name organizer]

Keywords:Fuel cell, Mass distribution, Cell performance, Flow rate, Over-potential

1. Introduction

Fuel cell technology, a core component in a hydrogen-based energy economy, has the advantages of high energy conversion efficiency, low pollution, and no dependency on depleting fossil resources.

1876–6102 © 2011 Published by Elsevier Ltd. Open access under CC BY-NC-ND license.
doi:10.1016/j.egypro.2011.05.008

Significant progress has been made in the state-of-the-art in materials, design, and fabrication; however, the widespread commercialization of most fuel cells is still limited by issues such as high cost and low durability [1, 2]. Mathematical models are effective tools in understanding and optimization of various transport and electrochemical processes, leading to cost reduction and improved performance and durability.

In the earlier stage of development, focus had been put on introducing new materials for various component of a SOFC [3, 4]. Active research efforts have been made recently to improve the understanding of the fundamental transport and electrochemical processes, aiming at optimal design and operation of the solid oxide fuel cells [1, 5]. With the availability of affordable and effective computational hardware and software, the trends of SOFC modelling moved toward multi-physics and multi-scale descriptions. Prinkey *et al.* [6] developed a computational fluid dynamics model. To describe the reactant flow, transport, and electrochemical reaction in a SOFC. Recknagle *et al.* [7] simulated the operation of a SOFC with three flow configurations: co-flow, counter-flow, and cross flow. A self-consistent SOFC model based on the single-domain framework was developed by Pasaogullari and Wang [8] to solve the conservation equations for mass, momentum, species, thermal energy and electric charge along with the electrochemical kinetics.

2. Performance model

The performance models characterize the electrical performance of a cell by using a single equation, *i.e.* cell voltage versus current density. The models are useful in determining kinetic parameters and general Ohmic resistance from experimental data [9]. However, the drawbacks of the performance models include the lack of fundamental description of mechanistic behaviour and detailed inner-cell operating conditions, which are critical for accurate prediction of cell performance or optimization. Accounting for various voltage losses, or over-potentials, involved in the operating of a fuel cell, a typical expression of the cell voltage, $U_{cell,}$ may be written in terms of the current density, *i,* as [10]. The voltage of a SOFC, $U_{cell,}$ is related to the open cell voltage, *E,* and various losses, η, [11]:

$$U_{cell} = E_{Nernest} - \eta_{Ohm} - \eta_{con} - \eta_{act} \tag{1}$$

Where the subscripts *Ohm., act.*, and *conc.* imply Ohmic, activation and concentration losses, respectively. The open circuit potential E_0 depends on the temperature and gas composition at the electrodes, and may be given by the Nernst equation

$$E_{Nernest} = E_0 - \frac{RT}{2F} \ln\left(\frac{p_{H_2O,f}}{p_{H_2,f}\, p_{O_2}}\right) \tag{2}$$

Where E_0 stands for the open circuit potential at standard temperature and pressure, *p* is pressure, and the subscripts *f* and *air* denote fuel and air channels, respectively. The voltage losses are associated with the electrochemical reactions at the three-phase boundary, and are affected by the temperature, pressure, gas flow-rate and composition, electrode/membrane materials, and cell designs. The losses consist of part the heat generation in an operating fuel cell. Furthermore, since both electrodes typically have high electrical conductivity, the cell voltage may be considered constant throughout the cell [12]. The Ohmic loss, η_{Ohm}, is caused by the resistance to the ion conduction through the electrolyte and electron conduction through

the electrodes and current collectors, and by the contact resistance between cell components. Ohm's law may be applied to relate η_{Ohm} to the current density, *i,* and the internal resistance, R_{Ohm} of the cell. Physical properties and parameters used in the present model are summarized in Table 1.

Table 1: Physical properties and parameters used [13]

Parameter	Value	Unit
Operating conditions		
Air inlet pressure, p	1	bar
Fuel inlet pressure, p	1	bar
Air inlet temperature, T	1073	K
Fuel inlet temperature, T	1073	K
Air flow rate	4.4.10-7	Nm^3/s
Fuel flow rate	7.9.10-8	Nm^3/s
Air utilization	21 % O2 + 79 % N2	
Fuel composition	97 % H2 + 3 % H2O	
Exchange current density	0.02	mA/cm^2
Cell length, L	0.1	m
Channel width, l	2.5	mm
Anode thickness, δ	500	µm
Cathode thickness, δ	50	µm
Electrolyte thickness, δ	10	µm
Anode porosity, ε	0.3	/
Cathode porosity, ε	0.9	/
Anode tortuosity, ζ	1.5	/
Cathode tortuosity, ζ	1.5	/
Thermal conductivity, σ of:		
Anode Ni-YSZ	2	W m-1K-1
Cathode, LSM	2	W m-1K-
Electrolyte, YSZ	2	W m-1K-1
Electric resistivity, ρ of :		
Anode	$2.98\times10^{-5}\,exp(-1392/T)$	Ω.m
Cathode	$8.11\times10^{-5}\,exp(600/T)$	Ω.m
Electrolyte	$2.94\times10^{-5}\,exp(10350/T)$	Ω.m

$$\eta_{Ohm} = iR_{Ohm} \tag{3}$$

The internal resistance may be obtained experimentally or be estimated from conductivity data and thickness of each layer.

$$R_{Ohm} = \sum \frac{\delta_m}{\sigma_m} \tag{4}$$

δ and σ represent the thickness and conductivity, respectively. Under open circuit conditions, the reactant and product concentrations at the three phase boundaries are equal to those in the bulk channel flow, and the Nernst equation, Eq. (2), predicts the open circuit potential. During cell operation with non zero current density, concentration gradients develop across the cell, resulting in lower concentration at the three-phase boundaries and concentration losses. The concentration losses may be expressed as [13]:

$$\eta_{con} = \frac{RT}{4F} ln\left(\frac{p^0_{O2}}{p^*_{O_2}}\right) + \frac{RT}{2F} ln\left(\frac{p^*_{H_2O} \cdot p^0_{H_2}}{p^0_{H_2O} \cdot p^*_{H_2}}\right) \tag{5}$$

To calculate the concentration losses, the relationship between the partial pressures at the three-phase boundary and the current density; i, must be determined. Considering the gas diffusion in the porous electrodes, the following expressions are obtained [14, 15]:

$$p^*_{H_2} = p^0_{H_2} - \frac{RT\delta_a}{2FD^{eff}_{an}} i \tag{6}$$

$$p^*_{H_2O} = p^0_{H_2O} + \frac{RT\delta_a}{2FD^{eff}_{an}} i \tag{7}$$

$$p^*_{O_2} = p - \left(p - p^0_{O_2}\right) exp\left(\frac{RT\delta_c}{4F\ pD^{eff}_c} i\right) \tag{8}$$

D^{eff}_a and D^{eff}_c are the effective diffusivities at the anode and cathode, respectively, and p is the total pressure. Slow reaction kinetics at the three-phase boundary leads to the activation losses, which are governed by the Butler-Volmer equation [13]:

$$i = i_0 \left[exp\left(\frac{\alpha\, n\, F}{RT} \eta_{act}\right) - exp\left(-\frac{(1-\alpha) nF}{RT} \eta_{act}\right)\right] \tag{9}$$

---

* : Three phase boundary

α is the transfer coefficient, n the number of electrons transferred in a single elementary rate-limiting reaction, and i_o *is* the exchange current density, [13].

3. Conservation equations

A fundamental description of fuel cell operation involves the conservation principles of mass, momentum, species and thermal energy. With a unified-domain approach, a set of governing equations valid for all the fuel cell layers may be written in the vector form as [16, 17]:

3.1. Mass transfer

Convective mass transfer plays an important role in the micro-channels, where the Navier-Stokes equations govern the velocity distributions. The species conservation equation is [18, 19, 20]:

$$\nabla.(\rho u X) - \nabla.(\rho D \nabla X) = \dot{S}_m \tag{10}$$

ρ is the mixture density **,** X is mass fraction , u is local velocity, D is the diffusion coefficient and $\dot{S}_m$ is a volumetric source term. Darcy's law may be applied to the porous electrodes

$$u = -\frac{k}{\varepsilon\mu}\nabla p \tag{11}$$

Mass transfer in the porous electrodes may be written in the same form as equation (10), but based on an effective diffusion coefficient D_{eff}, defined by:

$$D_{eff} = \frac{\varepsilon}{\zeta} D \tag{12}$$

At the interface between the electrodes and the electrolyte, the source/sink term per unit area, $\dot{S}_m$, for a given species (reactant/product) may be written as:

$$\dot{S}_m = \pm\frac{M}{nF} i \tag{13}$$

Where M is molecular number of electrons involved in the electrochemical reaction, F is Faraday's constant and *i* is the local current density at the interface

3.2. Heat transfer

Convective heat transfer is the dominant transfer mechanism in the micro channels, while conduction is important in solid materials [21, 22, 23]. For the electrochemical reaction,

$$H_2 + \frac{1}{2}O_2 \rightarrow H_2O \tag{14}$$

The total energy change resulting from the reaction is the difference in enthalpy of formation ΔH and Gibb's energy of formation ΔG [23], which is (theoretically) converted into electricity; the remaining is converted into heat. In reality, electrical (Ohmic) and activation losses, cause additional chemical energy to be irreversibly converted into heat (rather than electricity). Thus if U_{cell} is the operating voltage, the overall heat source may be written as:

$$S = i\left(\frac{\Delta H}{nF} - U_{cell}\right) \tag{15}$$

Equation (15) includes heat generated due to all sources. It does not however provide any indication as to how these terms are computed. Adiabatic boundary conditions are applied at the outer walls, i.e. all heat is removed by air and fuel. Inlet velocity values are determined from prescribed utilization rates for fuel and air; namely 25% for oxygen and 50% for hydrogen.

4. Numerical implementation

As shown in Fig. 1 a typical SOFC unit is symmetric about the mid-planes of the air and fuel channels. Therefore, the present computational domain covers the region between these two planes for memory and time saving. The governing equations were numerically solved by the control volume-based finite volume method [24]. The discretization procedure ensures conservation of mass, momentum and concentration over each control volume. The coupling of the pressure and velocity fields was treated via the SIMPLER pressure correction algorithm [25]. The upwind difference scheme was used to treat the convection and diffusion terms.

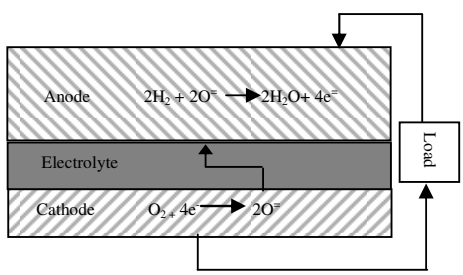

Fig.1. Governing electrochemical reactions for a solid oxide fuel cell

5. Results of the modeling studies

Two major groups of parameters are responsible for the overall cell performance, namely, the operating parameters, *e.g.*, temperature, pressure, gas composition and design parameters, *e.g.*, thickness of cell components. A good understanding of the effects of the design and operating conditions on the fuel cell performance is required to reduce the capital cost and improve the reliability. In this subsection, the effects of several critical parameters on the performance of a SOFC are first presented.

5. 1. Effect of operating pressure on SOFC performance

Under the simulation conditions listed in Nomenclature, and at typical temperature of 1073 K the effects of various operating pressure on the cell voltage is shown in Fig. 2. At high operating pressure 10 bar., the SOFC potential was found to decrease monotonically with increasing current density. At an operating pressure of 5 bar., the SOFC potential decreased slightly with increasing current density from 35000 to 40000 A/m^2 and then decreased slightly with a further increase in current density. This is due to the fact that the pressure contribution to the Nernst potential is logarithmic in nature.

5.2. Effect of fuel flow rate on the cell performance

Fig. 3 illustrates two calculated characteristics: *I–V* and *I*–power curves for the anode supported cell tests operating at 1073 K with gas flow rates of 80.10^{-9} and 80.10^{-8} m^3 s^{-1}, respectively. It reveals that only slight difference of current density for two different gas flow rates in the region of higher cell voltage while the differences expands the decrease of cell voltage. For gas flow rate of 80.10^{-8} m^3 s^{-1}, the peak power density was 37508Wm–^{2}, which was about 7.5 % higher than that of 80.10^{-9} m^3 s^{-1} gas flow rate.

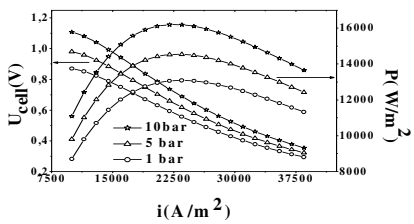

Fig.2. Effect of operating pressure on the cell performance

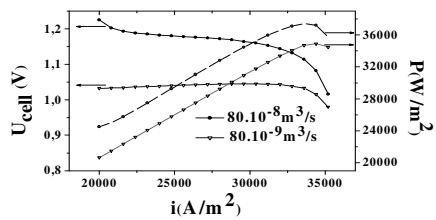

Fig.3. Effect of fuel gas flow rate on the cell performance

5.3.. Effect of various losses on the cell performance

Figs.4 and 5 illustrate the effect of various losses on the performance of fuel cell at an operating temperature of 873 K. It can be observed that, with the increase of loss term, cell potential decreases. This is attributed to the fact that, when the loss term increases, the source terms at the cell outlet decrease, hence the reversible cell potential decreases resulting in the decrease of actual cell potential.

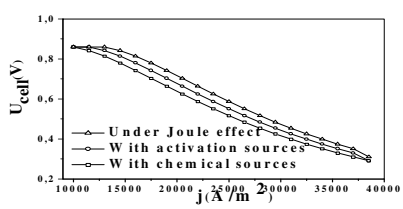

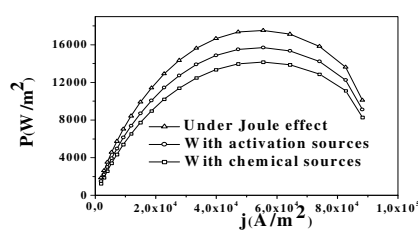

Fig. 4. Effect of various losses on the cell potential

Fig. 5. Effect of various losses on the cell performance

5.4. Effect of anode thickness

5.4.1. Hydrogen field

At the anode/electrolyte interface, in the anode middle the values of hydrogen mass decreases as the anode thickness increases, Table 2. H_2 mass does not reach the interface for the high anode thickness compared to the thin one Fig. 6. For all the anode thickness, hydrogen mass is located at the site situated in contact with the anode channel.

Table 2: Maximum rate of hydrogen consumed in anode

Anode thickness (μm)	300	500	1000
X_{H2} %	0.8192	0.7798	0.7220

The hydrogen mass transfer is from the anode channel to the interface with electrolyte. The mass transferred is high with weak anode thickness. The mass transfer according to the transversal direction is weak for the thin anode but more important and reached all the anode/electrolyte interfaces (1000μm).

5.4.2..Steam water field

Water localization is also influenced by anode thickness Fig. 7. The lowest value is obtained for high anode thickness. Table 3 shows that the maximum rate of created water fraction at the anode/electrolyte in the anode middle, the values of water fraction increases as the anode thickness increases. Water quantities produced at the interface are high. Water production becomes larger as the anode thickness increases. For the anode thickness values about 500–1000 μm all the interface contains water. As for the hydrogen and the water diffuses in the transversal direction in the case of a thicker anode and not in a case of a less thick anode. For both the H_2 and H_2O, the biggest mass quantities are at the middle anode. It becomes important at all the interface face at the thin anode thickness (300 μm).

Table 3: Maximum produced rate of steam water in anode/ electrolyte interface

Anode thickness (μm)	300	500	1000
X_{H2O} %	0.2087	0.1766	0.1470

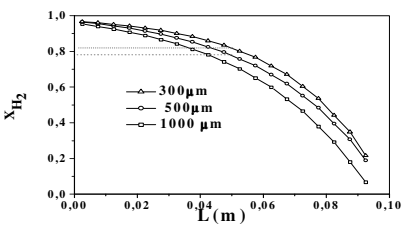

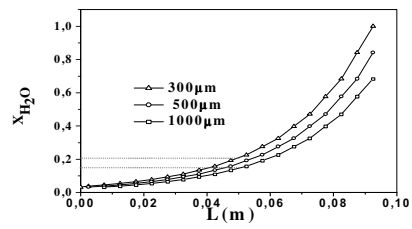

Fig.6. Hydrogen molar fraction distribution with different anode thickness values

Fig.7. Steam water molar fraction distribution with different anode thickness values

5.5. Temperature field under heat sources effect

Fig. 8 shows the temperature field for SOFC anode. On the whole, the fuel and air flow are progressively heated up by the heat generation due to the entropy change of the electrochemical reaction at the interface of anode and electrolyte. In the anode channel, the fuel mass flow rate is very small, so its velocity is very low, especially in the porous medium due to large resistance force. The results of a thermo-electrical model show the effect of various polarizations in the SOFC anode. Joule effect, heat due to the electrochemical reaction and that due to the activation losses are the results of the heat sources. The temperature increment in the anode of the cell is analyzed toward to parallel plan. According in the flow direction and for all the heat sources, the highest temperatures are in sites situated at the anode /electrolyte interface. These regions behave as a resistance to the heat propagation

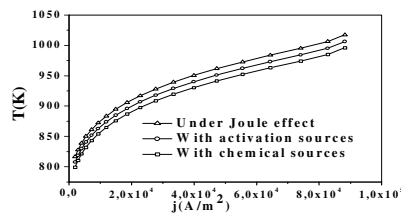

Fig.8. Temperature distribution under various over-potentials

On the other hand, the temperature became weak and this can be explained by the heat evacuation through anode and cathode gas flow channels. Under the Joule effect, the maximum temperature is obtained at the anode/electrolyte interface.

6. Conclusion

This paper has presented a computational simulation of the transport and electrochemical phenomena in a planar SOFC. Significant results about the local transport characteristics inside the planar SOFC, such as the steam water, hydrogen and the temperature distributions, under various losses, operating conditions and different values of thickness have been presented. The unique features of this model are the implementation of the voltage-to-current algorithm and the coupling of the potential field with the reactant species concentration field, which allows for a more realistic spatial variation of the electrochemical kinetics. The results of this numerical thermodynamic–electrical model, solved by finite volume method and resolved by self-programming (FORTRAN), [26] show the effect of the heat sources as the temperature changes. Furthermore, hydrogen mass transfer is function of the anode thickness. The

References

[1] D. Larrain et al, Generalized Model of Planar SOFC Repeat Element for Design Optimization. *J. Power. Sources 2004; 131:* 304–12.

[2] R.K. Shah, U.Desideri, K.L. Hsueh, A.V.Vikar Research Opportunities and challenges in Fuel Cell Science and Engineering. *The 4th Baltic Heat Transfer Conference Kaunas*. Proc. August 25–27, Lithuania, 2003.

[3] N.Q. Minh et al, Ceramic Fuel Cells, *J. Am. Ceram. Soc. 1993; 76*(3): 563–88

[4] B.Todd et al, Thermodynamic and Transport Properties of Gases for Use in Solid Oxide Fuel Cell Modelling. *J Power. Sources 2002; 110 :* 186–200.

[5] S. Dayadeep et al, Model development for a SOFC button cell using H_2S as fuel, *J. Power. Sources 2006; 162: 400-414.*

[6] M. Prinkey et al, Application of a New CFD Analysis Tool for SOFC Technology, *In Proceedings of IMECE* 2001; ASME: New York, 2001; Vol.369–4, p 291.

[7] K.P.Recknagle et al, Three-Dimensional Thermo-Fluid Electrochemical Modeling of Planar SOFC stacks. *J. Power. Sources 2003; 113:* 109–14.

[8] C.Y.Wang, Fundamental Models for Fuel Cell, *Engineering. Chem. Rev 2004; 104: 4727–66*.

[9] J.Pålsson, Thermodynamic *Modeling and Performance of Combined Solid Oxide Fuel Cell and Gas Turbine Systems,* Doctoral Thesis, Department of heat and power engineering. Lund University Sweden 2002.

[10] G. Squadrito et al, An Empirical Equation for Polymer Electrolyte Fuel Cell (PEFC) Behaviour. *J. Appl. Electrochem 1999; 29:1449–*55.

[11] J.Larminie et al, Fuel Cell Systems Explained. Wiley, West Sussex England, 2000.

[12] P. Aguiar et al, Anode-Supported Intermediate Temperature Direct Internal Reforming Solid Oxide Fuel Cell. I: Model-Based Steady State Performance, *J. Pow. Sources 2004; 138: 120-36.*

[13] L.Yixin, Numerical study of a flat-tube high power density solid oxide fuel cell Part I. Heat/mass transfer and fluid flow, *J. Power Sources 2005; 140: 331–39*

[14] L. Petruzzi et al, A Global Thermo-Electrochemical Model for SOFC Systems Design and Engineering. *J. Pow. Sources. 2003; 118:* 96–107.

[15] S.H.Chan et al, A Complete Polarization Model of a Solid Oxide Fuel Cell and Its Sensitivity to the Change of Cell Component Thickness, *J. Pow. Sources 2001; 93:*130–40.

[16] J.Kim et al, Polarization Effects in Intermediate Temperature, Anode-supported Solid Oxide Fuel Cells, *J. Electrochem. Soc 1999; 146:* 69–78.

[17] N. Autissier et al, CFD Simulation Tool for Solid Oxide Fuel Cells. *J.Pow. Sources 2004; 131: 313-19.*

[18] H.L.Anthony , *Mass Transfer Fundamentals and Applications*, Hall Inc.Englewood Cliffs, New Jersey, 1985, p. 46-7.

[19] A. Bejan, *Heat Transfer*, John Wiley & Sonc, Inc the United States of America, 1993.

[20] C.Haynes et al, 'Design for Power' of a Commercial Grade Tubular Solid Oxide Fuel Cell, *Energy Conversion and Management, 2000; 41:*1123–39.

[21] A.C.Burt at al, A numerical study of cell-to-cell variations in a SOFC stack, *J. Power. Sources 2004; 126: 76–87*

[22] R.T. Leah et al, Modelling of cells, stacks and systems based around metal-supported planar IT-SOFC cells with CGO electrolytes operating at 500– 600 ◦C, *J. Power. Sources 2005; 145: 336–52.*

[23] R.E.Sonntag et al, *Fundamentals of Thermodynamics. New* York: Wiley 1998.

[24] H.K. Verteeg et al, *An introduction to computational fluid dynamics the finite volume method,* Longman Group Ltd, 1995.

[25] S.V.Patankar, Numerical *heat transfer and fluid flow*, New York: McGraw-Hill Book Company; 1980.

[26] Hocine Mahcene et al. Study of species, temperature distributions and the solid oxide fuel cells performance in a 2-D model. Int. Journal of Hydrogen; 2010: 1-9.